Ultrasound in Med. & Biol. Vol. 17, No. 3, pp. 231–237, 1991
Printed in the U.S.A.

0301-5629/91 $3.00 + .00

Original Contribution

ULTRASOUND PROPERTIES OF LIVER WITH AND WITHOUT PARTICULATE CONTRAST AGENTS

T. A. TUTHILL,[†] R. B. BAGGS,[‡] M. R. VIOLANTE[*§] and K. J. PARKER[†*§]

[†]Department of Electrical Engineering, [‡]Departgment of Pathology, Division of Laboratory Animal Medicine,
[*]Department of Radiology, and [§]Rochester Center for Biomedical Ultrasound,
University of Rochester, Rochester, NY 14627, USA

(*Received* 29 *August* 1990; *in final form* 15 *November* 1990)

Abstract—Basic acoustic parameters are examined in rabbit liver with and without a solid contrast agent used for tumor detection. In normal liver, backscatter, attenuation, and sound speed are found to decrease with increasing water content. The addition of micron-sized particles made from iodipamide ethyl ester (IDE) can increase backscatter and attenuation depending on size and concentration. A discrepancy of the increased backscatter from theoretical predictions based on random scatterers is attributed to the particle's biodistribution in the liver.

Key Words: **Attenuation, Backscatter, Contrast agent, Lesion detection, Liver, Sound speed, Speckle, Tissue characterization.**

INTRODUCTION

Some encouraging initial results have been reported for a solid particle contrast agent in liver (Parker et al. 1987; Parker et al. 1990). Iodipamide ethyl ester (IDE) can be formulated with a narrow diameter distribution about a mean which can be selected within the range of 0.1 to 2.0 microns. The particles can be prepared under sterile conditions, are stable over time, and do not clump in the blood after intravenous injection. The circulating particles are then captured by the Kupffer cells which line the sinusoids of normal liver and the IDE is eliminated within two days. The high density (2.4 g/cm^3) of these particles, compared to surrounding tissue (1.0–1.1 g/cm^3), produces an impedance mismatch which is responsible for backscatter enhancement. Since tumors and other lesions lack Kupffer cells, they do not concentrate the particles and therefore would lack contrast effects compared to surrounding, normal tissue. In previous works we have reported some of the ultrasonic properties *ex vivo* of liver with IDE (Parker et al. 1987), and imaging results *in vivo* of rabbit liver implanted with VX2 carcinomas (Parker et al. 1990). This paper describes the measurement of ultrasonic backscatter, attenuation, and propagation of speed in rabbit liver with and without IDE particles. The changes in properties due to IDE uptake are related to those predicted by simple theories. The influence of biodistribution is examined. The results elucidate some of the underlying mechanisms of ultrasound propagation through normal liver and also underscore the importance of biodistribution in determining the ultrasonic effects of contrast agents.

THEORY

Backscatter

In the long wavelength approximation for scattering from an inhomogeneity of compressibility κ_s and density ρ_s in a fluid medium, the scattering cross-section, σ, is a function of the difference in material properties. It is also proportional to the frequency to the fourth power, and to the scatterer radius, a, to the sixth power. When a "cloud" of randomly positioned scatterers of concentration N per unit volume is present, the scattering cross-section, which is proportional to the total scattered power, simply increases with the concentration (Morse and Ingard 1968):

$$\sigma = N\frac{4\pi}{9}k^4a^6\left\{\left|\frac{\kappa_s-\kappa}{\kappa}\right|^2+\frac{1}{3}\left|\frac{3(\rho_s-\rho)}{2\rho_s+\rho}\right|^2\right\} \quad (1)$$

where k is the wave number, which is proportional to frequency and inversely proportional to wavelength. In the long wavelength approximation, the scatterer is assumed to be small, *i.e.*, $ka \ll 1$. A general discussion of this equation with respect to contrast agents is

given by Ophir and Parker (1989). For this current study, we examine the effects of dose, and also of particle size at constant dose, as predicted by eqn (1). The concentration of a substance in an organ is one of the primary variables in toxicity considerations. The concentration, D (gm of contrast agent per cm^3 of tissue), is related to the conventional variables as

$$D = N\left(\frac{4\pi}{3} a^3\right)\rho_s \tag{2}$$

and so we rewrite the scattering equation as

$$\sigma = \left(\frac{1}{3\rho_s}\right) Dk^4 a^3 \{\Delta z^2\} \tag{3}$$

where Δz represents the compressibility and density terms in brackets in eqn (1). This theoretical representation shows that scattered power will increase linearly with increased dose or concentration. Also, if the total dose is held constant but the particle radius is increased, the scattered power increases only as the cube of radius, not the sixth power as is commonly inferred from eqn (1). Assuming that the directionality of the scattering is independent of size in this long wavelength approximation, then for a constant dose, the RMS amplitude of a backscattered echo will increase with radius to the 3/2 power, a relatively modest increase.

Attenuation

The theory of relative motion has been used to describe the resulting wave propagation losses for the case where inhomogeneities are added to a viscous medium (Carstensen and Schwan 1959; Allegra and Hawley 1972). Density differences cause unequal displacement between particles and the surrounding medium during sinusoidal plane wave excitation. This relative motion, coupled with viscosity of the medium, generates a frictional loss per particle per acoustic cycle and thereby contributes to the overall attenuation coefficient. The attenuation is found to increase linearly with particle concentration and with the square of the density difference. The radius dependence is a complex function of frequency, though in general, the attenuation increases with size.

Speed of sound

Since the sound speed is directly related to density and compressibility, it will also be dependent on water content and particle concentration. Sehgal et al. (1986) apply a simple model, invoking perfect mixture rules (various components are assumed immiscible), showing the relationship of reciprocal sound speeds:

$$\frac{1}{c} = \frac{X_s}{c_s} + \frac{X_w}{c_w} + \frac{X_p}{c_p} \tag{4}$$

where c is the sound speed of the various components, X represents the volume fraction ($\Sigma X_i = 1$), and the subscripts, s, w, and p, are for "solid liver" component, water, and particles, respectively. IDE has a high speed of sound due to its density and incompressibility; thus, the overall liver sound speed should increase with particle concentration.

METHODS

IDE and rabbit liver preparations

The preparation for the solid, dense IDE particles has been described elsewhere (Parker et al. 1987). The particles were suspended in a saline solution for a final concentration of approximately 100 mg/mL.

In this animal study, New Zealand White rabbits (Hazelton Laboratories), weighing 2–4 kg, were anesthetized, and injected intravenously with a 10–15 mL (depending on weight) IDE suspension at a rate of 1 mL/min. At 2 h, the rabbits were sacrificed with a pentobarbital overdose, and their livers excised immediately and placed in chilled, degassed saline. During measurements, the livers were packed in a pill-box container, massaged to remove air bubbles, and secured by taut plastic wrap covers on the top and bottom thereby providing flat surfaces. All ultrasound measurements were done at room temperature and within 3 h of excision.

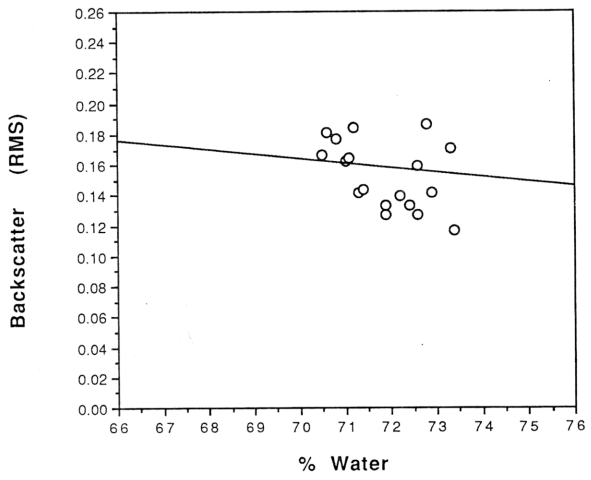

Fig. 1. Raw backscatter values (RMS) for normal rabbit livers plotted against water content. The solid line is from theory assuming the backscatter intensity is proportional to solid weight.

Backscatter

A pulse-echo technique was used to determine relative backscatter. A wideband, 10 MHz center frequency, Panametrics transducer (1.3 cm diameter, 5 cm focus), driven by a JSR Pulser, was used to obtain 8 RF scan lines from the anterior region of the right medial lobe. The stored data corresponded to 4 mm of tissue, starting at 1 mm below the surface to avoid ring-down effects. Precaution against specular reflectors was taken by monitoring the signal-to-noise ratio (SNR), and only saving scan lines where the SNR was greater than 1.5 (Tuthill et al. 1988). A standard deviation of 18% for the SNR is expected based on the properties of speckle.

Attenuation

Attenuation was measured by radiation force (Lyons and Parker 1986). The sample was placed between a narrowband transducer and a rubber absorber suspended from a Sartorius balance. The ultrasonic force on the absorber with and without the sample present determines the attenuation. By using the odd harmonics of three transducers, the frequency-dependent attenuation was computed over a range from 1 to 12 MHz. Errors less than 10% are expected using this technique.

Speed of sound

Velocity measurements were based on a time-of-flight technique using the same set-up as for backscatter measurements. The transducer was attached to a precision vernier and aligned perpendicular to the baseplate. Because of varying thickness in the liver samples, the device was first calibrated by measuring the arrival times of the baseplate echo in water for various transducer depths. By recording front and back echo times for the sample at known distances from the baseplate, both the thickness and sound speed could then be calculated at various sites. This technique provides accuracy errors less than 1%.

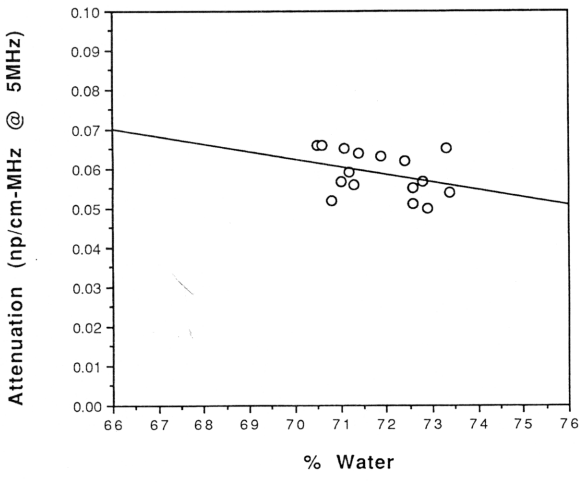

Fig. 2. Attenuation of normal livers at 5 MHz (divided by 5 MHz) plotted against water content. The solid line is the theoretical curve for attenuation being linearly proportional to solid weight.

Water content

To measure water content, three pieces ($\approx$0.5 g) were taken from each liver, cut into smaller pieces, and placed in glass containers to be weighed. The three samples were then heated at 90°C in a vacuum for 16 h, cooled in a desiccator, and reweighed. The weight loss then determines the water content. The accuracy is estimated as less than 1%.

RESULTS

The normal rabbit liver

The raw backscatter echo amplitude from 16 normal livers ranged from 0.12 to 0.18 mvolts, RMS, with an average of 0.15 mvolts (67 dB below the RMS echo from a perfect reflector). This large variation in normal values was found to be partly dependent on variations in the wet-to-dry weights of the liver specimens, as shown in Fig. 1. The solid line in Fig. 1 is a theoretical curve obtained by assuming that the backscatter (intensity) is linearly proportional to the solid weight of the liver, with zero backscatter at zero solid weight. The dependence of backscatter on water weight was noted by Bamber et al. (1981).

The results of attenuation measurements are given in Fig. 2, where the attenuation at 5 MHz is divided (or normalized) by 5 MHz to give α/f in np/cm-MHz. These data are plotted as a function of wet weight of the liver. The solid line is a theoretical curve where attenuation is assumed to be linearly proportional to solid weight. The specific absorption coefficient assumed in this line (α/concentration) is 0.207 np-cm^2/g-MHz, which is consistent with results of Kremkau and Cowgill (1984) and our earlier work on liver and glycogen (Lyons and Parker 1986; Parker et al. 1988; Tuthill et al. 1989).

The speed of sound plotted against water content for 9 normal livers is shown in Fig. 3. The mean value of 1580 $\pm$ 6 m/s is consistent with the literature values for different species (Bamber et al. 1981; Sarvazan et al. 1987) where the variability is explained by the wet-weight dependency. The solid line is the theoretical curve for simple mixture rules using reciprocal sound speeds, using 1490 m/s for water and 1570 for normal liver (72% water). This produces an intercept or "solid liver" value of 1860 m/s. Note that 1860 m/s is consistent with measurements of sound speed for materials with a high collagen (and low water) content (Johnston and Dunn 1976).

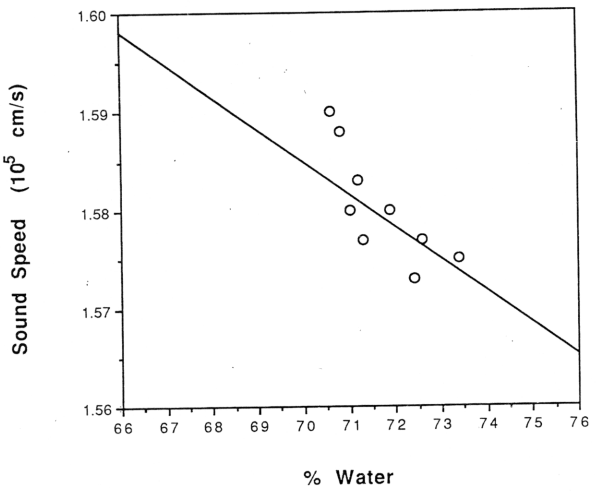

Fig. 3. Speed of sound for normal livers plotted as a function of water content. The solid line is the theoretical curve using perfect mixture laws (eqn 4).

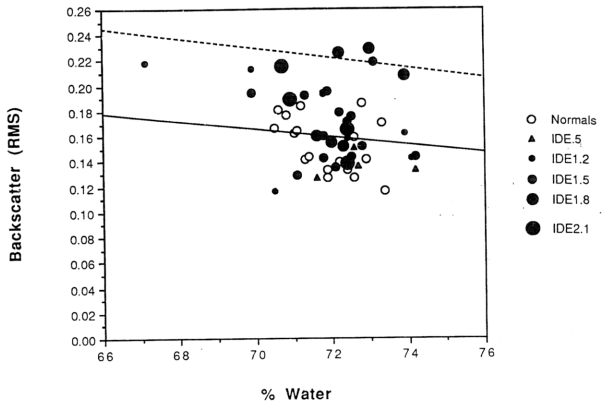

Fig. 4. Raw backscatter of all measured livers plotted versus water content. Open circles (○) represent normal livers, and solid symbols represent IDE livers for a range of doses and particle sizes. The solid line is the same as in Fig. 1. The dotted line is 3 dB above the solid line, representing a desirable increase in backscatter for lesion detection in speckle.

The normal liver with IDE

Data for liver with IDE, under experimental conditions covering a wide range of doses and particle sizes, are shown in Fig. 4. The same theoretical line as used in Fig. 1, normal (control) liver, is reproduced in Fig. 4 for comparison. The backscatter amplitudes are plotted as a function of water percentage to demonstrate that the average water content of IDE liver (mean value 72.1 ± 1.4%) is similar to that of control liver (mean value 72.0 ± 1.0%). This implies that no significant inflammatory reaction is initiated by the IDE, and thus any change in backscatter is due to the presence of the particles themselves, not to any change in the organ.

The backscatter from liver specimens containing IDE was studied as a function of dose and particle size. Figure 5 gives the results of backscatter versus particle size, where the mean IDE diameters ranged from 0.5 μm to 2.1 μm. (In these cases, the injected doses ranged from 4.4 to 7.2 mg IDE/kg body weight.) The data show that the 0.5 μm diameter IDE particles do not increase backscatter. In the 1.2–2.1 μm diameter range, an increase over controls is evident, but without a strong dependence of scattering on particle diameter as expected from theory. The effect of increasing concentration of IDE in the liver is shown in Fig. 6, where the final concentration, as measured from X-ray absorption techniques, ranges from 2.2 to 8.1 mg IDE/cc. (In Fig. 6, the 0.5 μm diameter particle results are excluded since they were shown to be ineffective for contrast, and only data from the 1.2–2.1 μm diameter IDE experiments are given.) The backscatter increases with concentration, as expected from theory, until a drop is seen at the highest concentrations. It was thought that increased attenuation at higher concentrations might be responsible for reducing the measured (uncorrected) backscatter. The IDE does increase attenuation, as shown in Fig. 7, and some increase with increasing IDE concentration would, in theory, be expected. However, when the backscatter results are corrected for attenuation, the results for experiments at the highest concentration (6–8 mg IDE/cc) still do not equal or exceed those at lower concentrations (3–5 mg IDE/cc). The significance of this, if any, is unclear.

To further eliminate experimental variability, the contrast enhancement of a single particle size (1.2 μm diameter) was studied over a narrow range of injected dose (200–300 mg IDE/cc), and evaluated as a comparison against control (normal) livers studied on the same day and chosen from the same group of

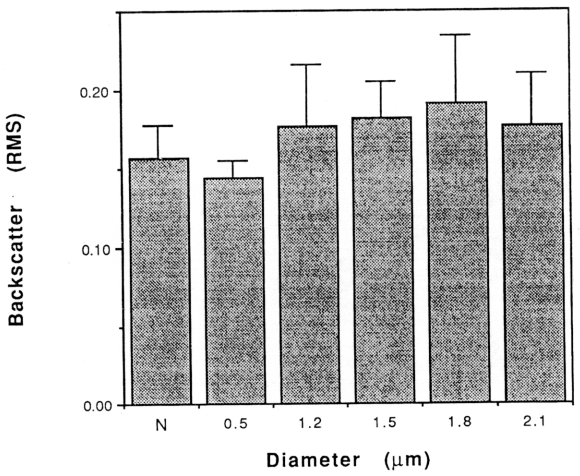

Fig. 5. Average backscatter (+1 SD) for normal livers and IDE livers with particle sizes ranging from 0.5 to 2.1 μ in diameter at a constant dose of 300 mg IDE/kg body weight.

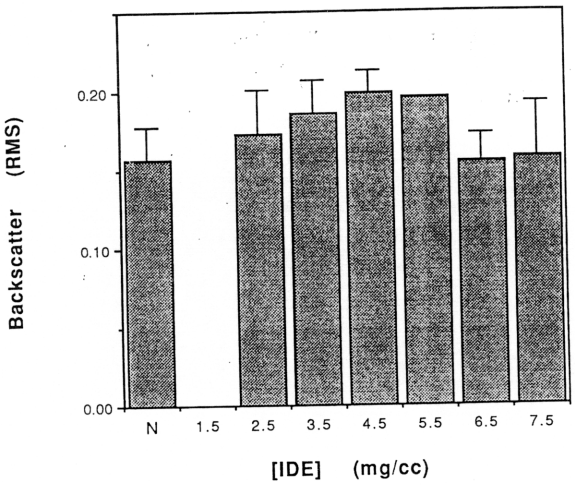

Fig. 6. Average backscatter (+1 SD) for livers with increasing concentration of IDE (mg/cc). The data represent particles sizes ranging from 1.2 to 2.1 μ.

rabbits. The results are given in Fig. 8, where the increased scatter due to IDE is expressed in percent above the control liver specimen backscatter. The results show an average increase of 30% (greater than 2 dB) for this dose and particle size.

For completeness, though the data is not given here, no significant change was found in the frequency dependence of liver backscatter with and without IDE. Also, the speed of sound in IDE liver did not differ from the controls, though this is to be expected as the total volume fraction of the IDE is less than 0.5%, and the increased sound speed would not be detected given measurement accuracies. In comparison, the increased backscatter at 3–4 mg IDE/cc liver (over a range of particle diameters, Fig. 6) and using 1.2 μm particles at 200–300 mg IDE/kg body weight (Fig. 8) were statistically significant at the $p < .05$ level.

Biodistribution

Within the last decade, some reports have indicated that the concentration of Kupffer cells is heterogeneous, the highest concentration being in the periportal region (Sleyster and Knook 1982). In addition, the periportal Kupffer cells have a higher endocytic activity. Our histology sections of IDE liver support this; a marked concentration of particles is observed within selected Kupffer cells that lie near the outflow of the portal triads. Figure 9 shows a stained histology section with a central vein at the center and portal triads near the periphery. The small, bright spots are aggregates of IDE particles within Kupffer cells. The brightness of the particles is due to their birefringent properties, as observed through crossed Nicol prisms. Visually, the bright spots are located away from the central vein, in a pattern which can be termed a peripheral lobular distribution. Examination by scanning electron microscopy shows that Kupffer cells capture up to 30 particles (Lauteala et al. 1984). Thus, a concentration of scatterers occurs at two levels. At the level of the Kupffer cells (scale approximately 10 μm), IDE is captured and held in groups of up to 30 particles. At the lobular level (scale approximately 1 mm), the IDE bearing Kupffer cells are concentrated in a peripheral lobular distribution. This pattern was observed over a range of doses (100–600 mg IDE/kg body weight) and particle sizes (1.2–2.1 μm diameter) in experiments in normal rabbit liver.

In other cases, where a VX2 carcinoma was implanted into the liver, a similar pattern was typically observed in tumor-free regions of the liver. Figure 10 is a histology section with a rapidly growing VX2 tumor on the right and liver parenchyma on the left. IDE particles appear as bright dots and are concentrated away from a central vein, despite the obvious distortion of the tissue in response to the tumor growth. The tumor region is virtually free of IDE, and this lack of uptake is responsible for the increased visibility of tumors (Parker et al. 1990).

DISCUSSION AND CONCLUSION

The normal rabbit liver properties are influenced by water content. The backscatter data show a trend towards decreasing echogenicity with increasing water content, as noted by Bamber et al. (1981). The attenuation is closely related to the specific absorption coefficient of large proteins, in agreement with the results of Kremkau and Cowgill (1984) and Tuthill et al. (1989). As water content increases, the attenuation and speed of sound decrease.

When IDE is added, there is no change in average water content. The resulting increase in backscatter

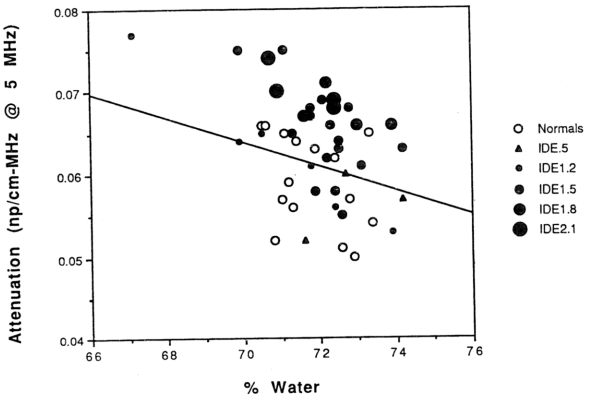

Fig. 7. Attenuation (divided by frequency) for all measured livers plotted versus water content. Open circles (○) represent normal livers, and solid symbols represent IDE livers for a range of doses and particle sizes. The solid line is the same theoretical line as in Fig. 2.

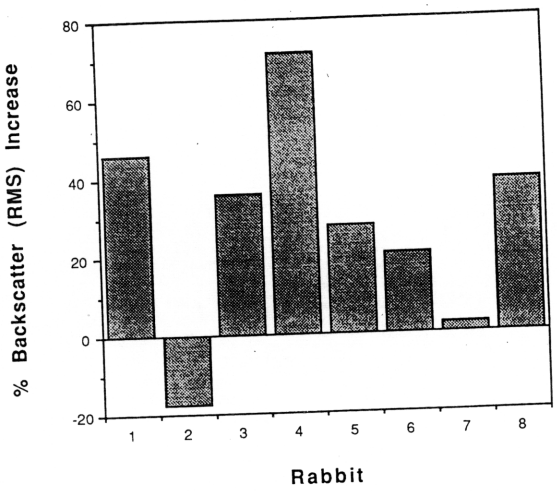

Fig. 8. Percent increases in backscatter of IDE livers over control livers from the same day. IDE rabbits were injected with 1.2 μ particles at doses between 200 and 300 mg/kg body weight.

depends on the particle size and dose administered and can be approximately a 3 dB increase in echo strength for 1.2 μm particles at 200–300 mg IDE/kg body weight. An increase of 3 dB is comparable to other backscatter variations which have been utilized in tissue characterization such as those associated with myocardial tissue (Mottley and Miller 1988). Furthermore, 3 dB is a significant enhancement in regards to the lesion detection problem for fully developed speckle (Lowe et al. 1988; Sperry and Parker 1990). This enhancement may be increased further by changing the density and compressibility properties of IDE in future research.

It must be emphasized that the backscatter does not follow the simple superposition of normal liver plus the addition of randomly positioned, single particles of IDE. There is not, as theory predicts, a strong dependence on particle size. There is not, as theory predicts, a monotonic increase with dose. Furthermore, the overall increase is larger than would be expected from preliminary *in vitro* studies of IDE suspensions in gelatin, which would predict a 1 dB increase for 1.2 μm particles at a final concentration of 5 mg IDE/cc, instead of the 3 dB observed.

Presumably, the explanation for these gross discrepancies lies with the concentration effects by the Kupffer cells in the peripheral lobular regions. The effect of this biodistribution on scattering is not known theoretically, but will be addressed using mathematical models and the optical staining-transform methods of Waag et al. (1983).

Also, the accumulation of IDE particles in the presence of a tumor needs to be examined. Kupffer cells are known to surround tumor cells in their early stages (Wake et al. 1989), though as the tumor grows this process is blocked by tumor cell products. This initial encirclement may produce a ring of IDE particles and further enhance the contrast between tumor and healthy tissue.

The mechanisms which produce a distinct peripheral lobular distribution of particles are not fully understood and will require further research. Presumably the pattern of particle acquisition will be germane to other classes of dense, solid particles, which may be formulated for x-ray or MRI image enhancement. Thus, the biodistribution effects may prove im-

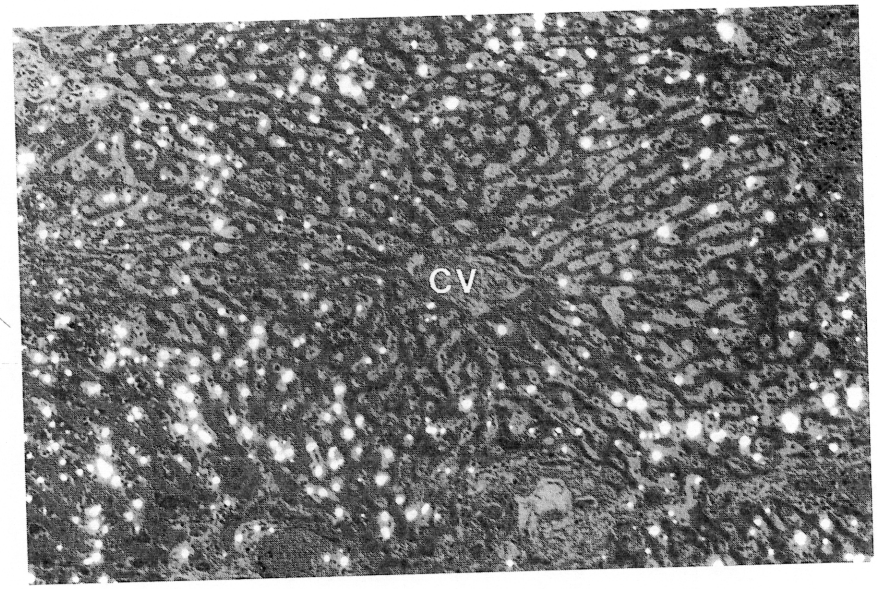

Fig. 9. Stained histology section of a normal liver lobule injected with IDE (bright spots). The central vein is in the center, and the portal triads are near the periphery.

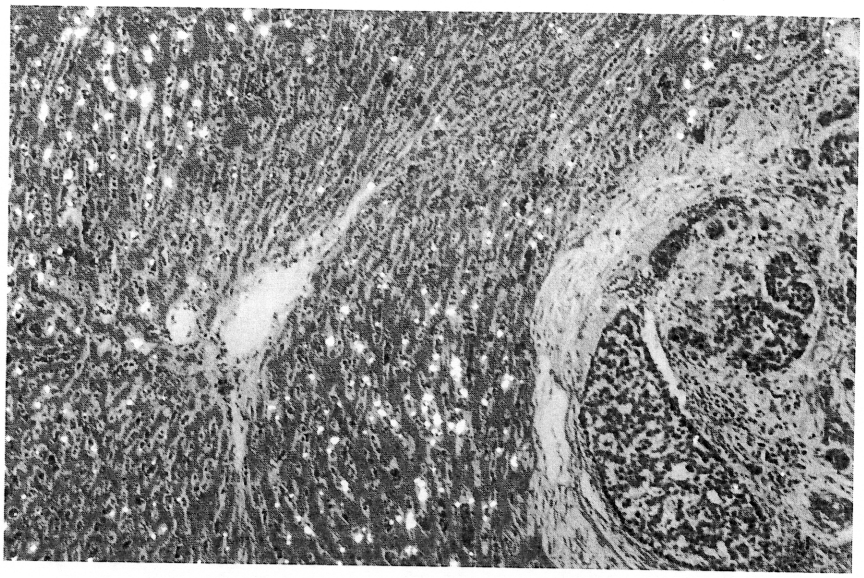

Fig. 10. Stained histology section of a cancerous liver injected with IDE. On the left is normal tissue, and on the right is a VX2 tumor.

portant to other imaging modalities in addition to ultrasound.

Acknowledgements—This work was supported by NIH grant no. CA44732. We are also grateful for the expert experimental assistance of Mr. P. Dentinger and Ms. D. Hartley.

REFERENCES

Allegra, J. R.; Hawley, S. A. Attenuation of sound in suspensions and emulsions: Theory and experiments. J. Acoust. Soc. Am. 51:1545–1564; 1972.

Bamber, J. C.; Hill, C. R.; King, J. A. Acoustic properties of normal and cancerous human liver—II Dependence on tissue structure. Ultrasound Med. Biol. 7:135–144; 1981.

Carstensen, E. L.; Schwan, H. P. Absorption of sound arising from the presence of intact cells in blood. J. Acoust. Soc. Am. 31:185–189; 1959.

Johnston, R. L.; Dunn, F. Influence of subarachnoid structures on transmeningial ultrasonic propagation. J. Acoust. Soc. Am. 60:1225–1227; 1976.

Kremkau, F. W.; Cowgill, R. W. Biomolecular absorption of ultrasound I. Molecular weight. J. Acoust. Soc. Am. 76:1130–1135; 1984.

Lauteala, L.; Komano, M.; Violante, M. Effect of IV administered IDE particles on rat liver morphology. Invest. Radiol. 19:133–141; 1984.

Lowe, H.; Bamber, J. C.; Webb, S.; Cook-Martin, G. Perceptual studies of contrast, texture, and detail in ultrasound B-scans. SPIE Medical Imaging II 914:40–47; 1988.

Lyons, M. E.; Parker, K. J. Absorption and attenuation in soft tissue I—Calibrations and error analysis. IEEE Trans. Ultrason., Ferro., and Freq. Control UFFC-35:242–252; 1986.

Morse, P. M.; Ingard, K. U. Theoretical acoustics. New York: McGraw-Hill, Inc.; 1968:427.

Mottley, J. G.; Miller, J. G. Anisotropy of ultrasound backscatter of myocardial tissue I: Theory and measurements *in vitro*. J. Acoust. Soc. Am. 83:755–761; 1988.

Ophir, J.; Parker, K. J. Contrast agents in diagnostic ultrasound. Ultrasound Med. Biol. 15:319–333; 1989.

Parker, K. J.; Tuthill, T. A.; Lerner, R. M.; Violante, M. R. A particulate contrast agent with potential for ultrasound imaging of liver. Ultrasound Med. Biol. 13:555–566; 1987.

Parker, K. J.; Tuthill, T. A.; Baggs, R. B. The role of glycogen and phosphate in ultrasound attenuation of liver. J. Acoust. Soc. Am. 83:374–378; 1988.

Parker, K. J.; Baggs, R. B.; Lerner, R. M.; Tuthill, T. A.; Violante, M. R. Ultrasound contrast for hepatic tumors using IDE particles. Invest. Radiol. 25:1135–1139; 1990.

Sarvazyan, A. P.; Lyrchikov, A. G.; Gorelov, S. E. Dependence of ultrasonic velocity in rabbit liver on water content and structure of the tissue. Ultrasonics 25:244–247; 1987.

Sehgal, C. M.; Brown, G. M.; Bahn, R. C.; Greenleaf, J. F. Measurement and use of acoustic non-linearity and sound speed to estimate composition of excised livers. Ultrasound Med. Biol. 12:865–874; 1986.

Sleyster, E. C.; Knook, D. L. Relation between localization and function of rat liver Kupffer cells. Lab. Invest. 47:484–490; 1982.

Sperry, R. H.; Parker, K. J. Segmentation of speckle images based on level crossing statistics. J. Opt. Soc. Am. 18:490–498; 1991.

Tuthill, T. A.; Sperry, R. H.; Parker, K. J. Deviations from Rayleigh statistics in ultrasonic speckle. Ultrasonic Imaging 10:81–89; 1988.

Tuthill, T. A.; Baggs, R. B.; Parker, K. J. Liver glycogen and water storage: Effect on ultrasound attenuation. Ultrasound Med. Biol. 15:621–627; 1989.

Waag, R. C.; Nilsson, J. O.; Astheimer, J. P. Characterization of volume scattering power spectra in isotropic media from power spectra of scattering by planes. J. Acoust. Soc. Am. 74:1555–1571; 1983.

Wake, K.; Decker, K.; Kirn, A.; Knook, D. L.; McCuskey, R. S.; Bouwens, L.; Wisse, E. Cell biology and kinetics of Kupffer cells in the liver. Int. Rev. Cytol. 118:173–229; 1989.